

AVOID: The Adverse Visual Conditions Dataset with Obstacles for Driving Scene Understanding

Jongoh Jeong^{2,*}, Taek-Jin Song^{1,*}, Jong-Hwan Kim¹ Kuk-Jin Yoon²,
Robot Intelligence Technology Lab.¹, Visual Intelligence Lab.², KAIST

tjsong@rit.kaist.ac.kr, {jeong2, kjyoon}@kaist.ac.kr, johkim@rit.kaist.ac.kr*

Abstract

Understanding road scenes for visual perception remains crucial for intelligent self-driving cars. In particular, it is desirable to detect unexpected small road hazards reliably in real-time, especially under varying adverse conditions (e.g., weather and daylight). However, existing road driving datasets provide large-scale images acquired in either normal or adverse scenarios only, and often do not contain the road obstacles captured in the same visual domain as for the other classes. To address this, we introduce a new dataset called AVOID, the Adverse Visual Conditions Dataset, for real-time obstacle detection collected in a simulated environment. AVOID consists of a large set of unexpected road obstacles located along each path captured under various weather and time conditions. Each image is coupled with the corresponding semantic and depth maps, raw and semantic LiDAR data, and waypoints, thereby supporting most visual perception tasks. We benchmark the results on high-performing real-time networks for the obstacle detection task, and also propose and conduct ablation studies using a comprehensive multi-task network for semantic segmentation, depth and waypoint prediction tasks¹.

1. Introduction

Visual understanding of urban scenes has been a growing field of research across academia as well as industry. In particular, the automation and its applications for fully autonomous vehicles have gained significant attention with a wide availability of urban street datasets with high-quality annotations for tasks such as semantic segmentation and depth estimation. More specifically, visually recognizing small, unexpected road hazards is a key issue in real-world driving scenarios in which unanticipated objects may interfere with the traffic at any given time and weather condition,

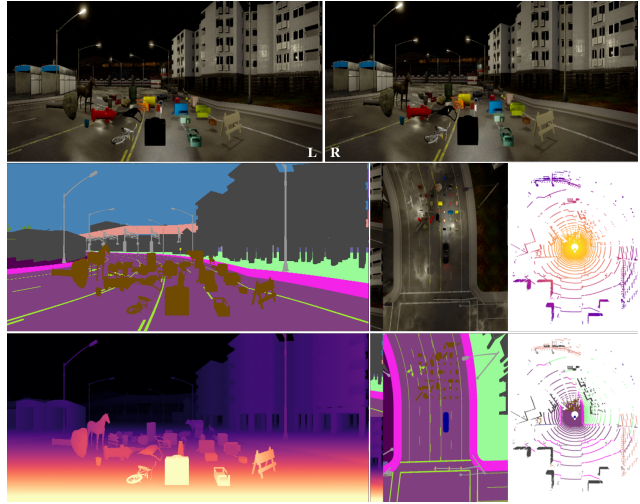


Figure 1. Sample views of all obstacles in AVOID. AVOID provides a set of multi-view images and annotations for each observed driving scene. As the vehicle navigates through the simulated routes, it collects a stereo pair of egocentric RGB images (top row) and the corresponding annotations (semantic and depth maps, RGB and semantic maps in Bird’s-Eye-View (BEV), and raw and semantic LiDAR data, shown from left to right on bottom two rows)

leading to high collision risks. Moreover, the cases of failure to detect road debris on the highway have recently been on the rise, with about 1.3 million road traffic death tolls every year [42, 47, 73], which the UN General Assembly has even set forth a plan to halve by 2030 [2]. Such road hazards are usually varied in size, shape, texture, and color, and tend to appear abruptly without clear hints in advance. Considering the safety of vulnerable road users including pedestrians, cyclists, and motorcyclists, these characteristics entail even greater significance in detecting unexpected road obstacles.

Objects in a driving scene, including obstacles, are encountered on the road not only during normal conditions, but also in “unusual road or traffic conditions that [are] not

*Taek-Jin Song and Jongoh Jeong contributed equally to this work.

¹Dataset will be released to public at [weblink].

known” [23], i.e., adverse driving conditions. Such conditions, including adverse weather (*e.g.*, rain) and daytime (*e.g.*, night), pose serious threats to road users and vehicles as they deteriorate desired lighting conditions for better visual perception and often incur driver fatigue [5]. For instance, rainfall yields as high risk of crashes as 70% compared to clear weather due to wet roads [1]. Lighting, despite rarely being a direct cause of collisions, do compound more direct causal factors for driver fatigue by impeding the visual reaction time, thereby increasing stopping distance [5, 68]. For self-driving applications, perceiving class-agnostic road hazards under these adverse conditions is thus of critical importance for the safety of both intelligent agents and practical road users.

To that end, we propose a novel simulated driving dataset containing on-road obstacles of various characteristics and the corresponding high-quality annotations from diverse sensor inputs. While there are a number of synthetic (simulated) and real-world datasets under adverse environmental settings only [13, 32, 62], there is yet no single comprehensive obstacles dataset in such conditions that provides various output modalities including paired stereo images, semantic and depth maps, and raw and semantic LiDAR sensor data. Several previous works [58, 67], on the other hand, address the task of detecting small unexpected on-road obstacles by opting to fuse two different segmentation datasets in similar real-world road driving domains, but only in clear weather. We thus introduce a novel obstacles dataset under various adversarial scenarios in a simulated environment for use in most visual perception tasks including semantic segmentation. Note that the obstacles in our dataset as seen in Fig. 1 are ones encountered commonly on the road and we exploit the CAR Learning to Act (CARLA) simulator [20] to realize various scenes that are otherwise not feasible for data collection in real worlds due to physical resource and societal costs.

We highlight our contributions in three-fold as follows:

1. We introduce a novel large-scale dataset for obstacle detection under adverse environmental conditions, collected in a simulated environment. Our dataset provides high-quality annotations for use in most visual perception tasks that require RGB, Depth and LiDAR as inputs.
2. We provide benchmark results on the obstacle detection task under 42 different adverse conditions on high-performing single-task networks for the semantic segmentation and waypoint prediction tasks.
3. We examine the performance of a real-time, lightweight obstacle detection network on our proposed dataset for road navigation using a transformer-based feature fusion approach, achieving up to 51.81% IoU in obstacle detection (ResNet-18 backbone) at 18.87 FPS on a single Nvidia RTX 3090 GPU.

2. Related Work

Unexpected small on-road obstacle detection. The task of detecting unexpected on-road obstacles deals with identifying never-seen-before objects from the semantic segmentation map in a driving scene. As it is a time- and safety-critical task that requires efficient, real-time processing in practice, a number of proposed vision-based comprehensive systems [29, 41, 54] have thus incorporated various image views, such as passive vision, frontal and rear-view images and shadows of objects on the road. Similar to several other obstacle detection works in light of anomaly detection [16, 35, 38, 46] based on resynthesis, a restricted Boltzmann machine and an uncertainty-based model, these systems, however, merely target detecting the presence of obstacles in the free space in front or at the back of the vehicle, in addition to detecting other vehicles and pedestrians.

It is, yet, of paramount importance to identify and localize *unexpected* on-road obstacles of various characteristics (*e.g.*, size, shape, and texture) at pixel-level from the segmentation map, in particular, those at a long distance range for timely response to potential road hazards [51, 52]. For safety-critical moving platforms like self-driving vehicles, this task thus remains a key component that can further minimize traffic collisions due to undesirable road debris and obstacles. To that end, traditional filtering- [25] and recent deep learning-based [37, 63] approaches have been proposed to distinguish relevant objects from the irrelevant ones in a driving scene using image inputs.

Using a Light Detection and Ranging (LiDAR) sensor that has recently gained attention as a standard sensor for various autonomous driving tasks, [36] introduces the Stixel representation of vertical strips in the RGB image and [72] dynamically selects the threshold parameters for an improved DBSCAN clustering for obstacle detection. However, LiDAR sensors incur significant physical maintenance and computational overheads, and thus many other works have instead opted to use cost-effective RGB and depth sensors together in cross-modal learning [15, 22]. In particular, [53, 69] demonstrate the advantage of contextual learning across data modalities using semantic and geometry cues for obstacle detection from the segmentation map. Further, [67] achieves higher detection performance without the depth input by refining the predicted semantic and disparity maps in a single stage.

Driving datasets in adverse conditions. Apart from employing different sensors for more comprehensive understanding of a scene in an adverse environment, the quantity and quality of vision datasets for self-driving primarily determine the predictive performance of an intelligent driving agent. For the task of semantic segmentation, a task of classifying each pixel in an image into its representative category among the pre-defined set of classes, KITTI [24] and Cityscapes [14] datasets have sparked sig-

nificant progress in learning-based visual recognition in the real domain given RGB camera and LiDAR sensor inputs. Following the two seminal ones, a number of other datasets aimed at increasing in scale have demonstrated the difficulty of acquiring high-quality pixel-level annotations by hand [28, 45], and accordingly, synthetic datasets of even larger scales [30, 56, 57] have shown to be advantageous in collecting and annotating the ground truth data automatically.

Several simulator-based [13, 19] explicitly exploit the use of the CARLA simulator [20] on the Unreal Engine for simulating visual road navigation in an adverse environment set by the pre-defined environmental parameters. Other works synthetically generate adverse conditions by applying the fog density by adjusting the control parameter, β [60], and use a generative model to adapt from clear to adverse weather conditions [59]. However, most datasets including Foggy Driving [60], Foggy Zurich [17], Nighttime Driving [18], Dark Zurich [61], Raincover [74], WildDash [80] and BDD100K [79] aimed at semantic labelling in adverse conditions (e.g., fog, night, rain and snow) merely contain fewer than a thousand images, with [79] being the only exception with 1,346 images but with severe errors. A more recent [62] contains an equally distributed set of real-world adverse condition images following the same four adverse classes at a larger scale, and [13] is only trained with coarse semantic labels with the primary task being road navigation. To address the limitations of existing adverse conditions datasets from the obstacle detection perspective [4, 31, 44, 50, 66], our dataset provides a more diverse and large-scale sensor input data acquired in the same visual domain, and the corresponding pixel-level class-agnostic obstacle annotation, together with the other benchmark classes.

3. AVOID Dataset

We follow the design principles, and the data collection and annotation strategies established by the well-received semantic segmentation datasets [14, 62] to target our primary task, obstacle detection, as well as by the seminal simulator-based datasets for road navigation [13, 19, 20] to realize and collect more practical data under adverse condition scenarios.

Motivation. With the growing demand for driving scene datasets that target domain shifts from synthetic and real datasets, driving scene datasets under adverse conditions are becoming essential. However, only a few such datasets containing road obstacles are available in real-world settings due to practical concerns in data collection, let alone in simulated environments. In light of the success of recent CARLA simulator-based road navigation datasets under adverse conditions [13, 19] that provide multiple output modalities including LiDAR and RGB, we thus build upon

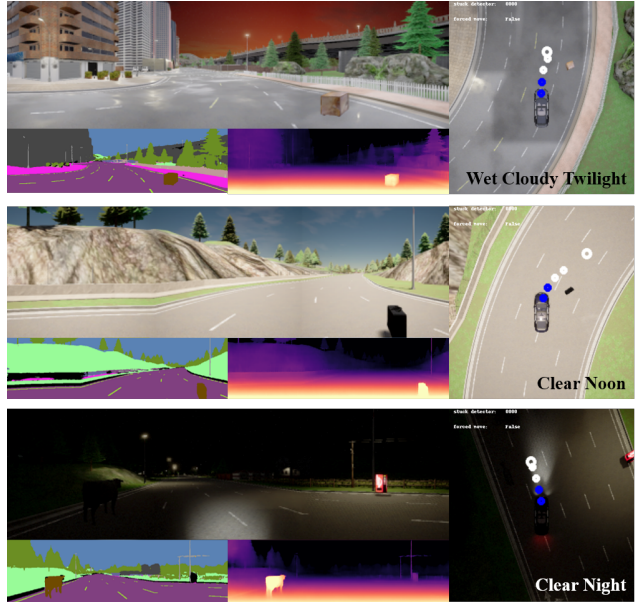


Figure 2. Samples results of the vehicle avoiding obstacles ahead (a nightstand, a black suitcase, and a black cow, from top to bottom in order).

their works to introduce class-agnostic obstacles of various sizes, shapes, textures, and categories to the provided town routes in CARLA. In common visual perception tasks for road navigation, unknown obstacles are bound to appear in unanticipated time, place and occasions without hints, thereby restricting intelligent driving agents in both navigating planned routes and safely avoiding unexpected objects appearing in their fields-of-view. As fully autonomous vehicles are becoming rapidly commercialized, detecting unexpected obstacles as small as 5 cm in height [58, 67] is a key specification that needs to be met in practical road driving scenarios.

Approach. A common approach to collecting an urban scene driving dataset with road obstacles is by simulating a driving environment virtually as considerable costs in physical resources, time, personnel and safety are inevitably associated with collecting real-world road scenes containing diverse on-road obstacles. The Town05 CARLA dataset [13] is one that is collected through simulated navigation and evaluated by taking simulated RGB images and LiDAR data as inputs to their multi-modal fusion transformer network to encourage global contextual learning across different data modalities.

While their data collection strategies include variations in weather and daylight conditions divided into 36 different adversarial conditions following [12], and using multi-modality sensors to precisely describe the scene, Chitta *et al.* overlook the unrealistic settings in the collected scenarios in which the environmental condition is altered at

Table 1. Comparison of AVOID against clear and adverse environmental condition semantic segmentation datasets

Dataset	Env.	Condition	Modality	Semantic Annotation		Depth Map		Waypoints	Resolution	# Frames	
				# Classes	Obstacle	Acquisition	Precision			Train / Val. / Test	
Cityscapes [14]	Real	Clear	Stereo RGB	Fine (19)	✗	SGM [26]	-	✗	2048×1024	5,000 (2,975 / 500 / 1,525)	
Lost and Found [52]		Clear	Stereo RGB	Coarse (3)	✓	SGM [26]	-	✗	2048×1024	2,239 (1036 (train/val.) / 1203)	
ACDC [62]		Adverse	Monocular RGB	Fine (19)	✗	N/A	-	✗	1920×1080	4,006 (1,600 / 406 / 2,000)	
TransFuser [13]	Sim.	Adverse	Monocular RGB	Coarse (7)	✗	Depth camera	FP24 [20]	✓	960×160	226,889 (168,159 / 58,730 / -)	
SHIFT [71]		Adverse	Stereo RGB	Fine (23)	✗	Depth camera	FP24 [20]	✓	1280×800	2.5 M	
AVOID (Ours)		Adverse	Stereo RGB	Fine (17)	✓	Depth camera	FP24 [20]	✓	960×320	21,403 (17,792 / 2,477 / 1,134)	

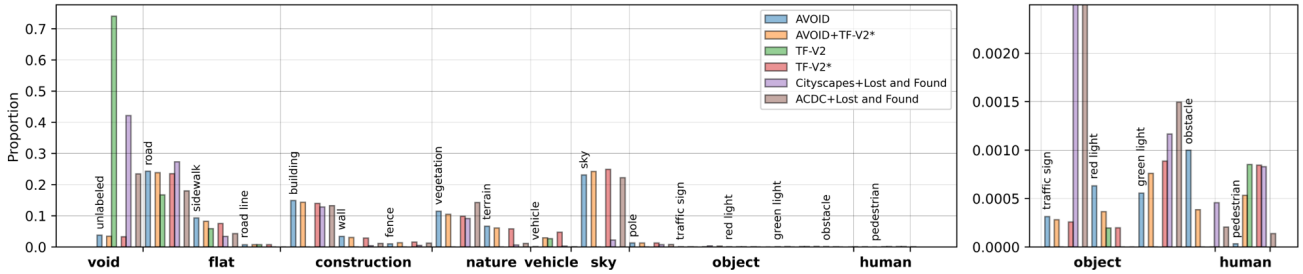


Figure 3. Comparison of data distributions for pixel-wise semantic labels across the segmentation datasets.

every frame during the data collection process. Moreover, *clear* weather is omitted to evaluate specifically under the select CARLA’s adversarial scenarios 1,3,4,7,8,9,10 generated according to the NHTSA pre-crash typology, such as lane merging and changing, as well as negotiations at traffic intersections and roundabouts, as per the CARLA Autonomous Driving Challenge scenarios².

We thus introduce a new dataset called AVOID, the Adverse Visual Conditions Dataset, that builds upon the previous CARLA-based one [13] for better scene perception by providing a more comprehensive set of annotations that are acquired with time synchronization (e.g., paired stereo images, semantic LiDAR data, and additional pixel-level semantic class labels). Building upon the code [7] based on the handcrafted rules and guided by the collection principles by the authors of [13], we carried out an expert policy provided by the CARLA simulator which allows the vehicle to navigate with the privileged ground truth waypoint labels. These waypoints set by the simulator are then navigated through the Towns as shown in Fig. 4 using an A* planner followed by two independent PID controllers in the lateral and longitudinal directions. The high-quality pixel-level annotations for the sensor outputs, including paired stereo RGB images, semantic and depth maps, and raw and semantic LiDAR data, have been auto-labeled by the simulator. We highlight the improvements as follows: (1) addition of *clear* weather condition, yielding 42 different weather-daytime combinations, (2) fixed adversarial environment for each scenario for more realistic environmental changes, rather than altering on a frame-by-frame basis, (3)

inclusion of the *obstacle* semantic class, (4) synchronized stereo RGB image pairs in a panoramic view (stitched *Left*, *Focus* (Center), *Right* views with each camera FoV=60° and baseline distance 0.2m apart), and (5) more diverse data modalities including paired RGB and semantic LiDAR acquired synchronously. Detailed comparison across related datasets and annotation statistics are presented in Table 1 and Fig. 3, respectively.

Obstacles. We acquired 45 different 3-D object models of various textures, shapes and sizes in FBX format from the web³, including those belonging to categories ranging from *Nature*, *Construction*, *Transport Artifact*, *Container* and *Animal* to *Other* (See *Supplementary* for detailed description of objects). We specifically selected objects that are encountered commonly on-the-road, roadside, and random items that may fall from cargo trucks from behind.

For each imported object, we manually applied transforms (e.g., translation, rotation, uniform scaling) to fit to the road environment. For example, a fire hydrant object was uniformly scaled by 1.8, translated by (0,0,25) and rotated by (0,90,-60) tuning parameters. The object positions on the path were set according to (1) whether the vehicle travel path is heavily interrupted due to the object at the intersection, for instance, (2) whether the vehicle can safely follow the waypoints around the object, and (3) if the vehicle encounters the object at some distance into straight or curved roads. We accordingly set the waypoints for the vehicle to avoid obstacles as follows: (1) using the obstacle detector in CARLA, vehicle is notified of the obstacle at 10

²<https://leaderboard.carla.org/scenarios>

³FBX (.fbx) is a file format for high-fidelity 2D and 3D geometry and animation data, widely used in film, game, and AR / VR development.

meters in distance, (2) waypoints to circumvent the obstacle are manually set such that they are 3 meters away from the obstacle, and (3) straight waypoints in the forward direction after avoiding the obstacle are set after the vehicle is 5 meters apart from the passed obstacle. The type of obstacle for each path in a scenario is randomly determined for more realistic considerations as well as convenience. We note that this simulation environment can be further expanded by customizing with objects of the user’s interest. We visualized in Fig. 2 sample road navigation views in which the ego-centric vehicle avoids the obstacle in its frontal view by circumventing it.

3.1. Data Specifications

Our data collection process is automated in CARLA [20] 0.9.11 simulator which provides eight publicly available town maps. We take advantage of the CARLA environment for its customize-able weather and temporal parameters in simulated self-driving scenarios. We further detail these adverse condition parameters in *Supplementary*.

Throughout the path routes, our data collection process was synchronized in time for all resulting RGB and LiDAR data. In the simulated environment, we set the LiDAR sensor parameters {Dropoff General Rate=0, Dropoff Intensity=10, Dropoff Zero Intensity=0} in order to match the raw and semantic LiDAR data for each frame. For the RGB camera, the baseline distance, field-of-view, and the width are set to 0.2 meters, 60°, 320 pixels, respectively. The maximum visible depth range in an acquired image is thus 55.4 meters, according to focal length $f = (width/2)/\tan(FoV/2)$ and the epipolar geometry equation for depth and disparity.

For safe navigation by avoiding obstacles, we intended to allow the vehicle to cross the center yellow line upon encountering an obstacle by manually setting waypoints accordingly. In this approach, we limited the appearance of pedestrians and other vehicles in the dataset in order for the vehicle not to confuse with or stop abruptly in front of people and vehicles. We note that this pre-defined setting resulted in relatively lower numbers of the two classes compared to those in [13]. Moreover, the image height is experimentally determined to be twice that of the TransFuser as the field-of-view is significantly restricted, or cut out, for our panoramic view of 960×320 resolution when a pedestrian of short height or small obstacles appear. During navigation, the vehicle is also set to stop and remain idle if it detects a red traffic light within its driving angle of 60° or 7 meters in distance.

Adverse Environmental Conditions. AVOID involves 7 different weather (Clear, Cloudy, Wet, Wet-Cloudy, Hard-rain, Mid-rain, Soft-rain) and 6 different daytime conditions (Night, Twilight, Dawn, Sunset, Morning, Noon), totaling 42 unique adverse conditions that are realized per scenario.

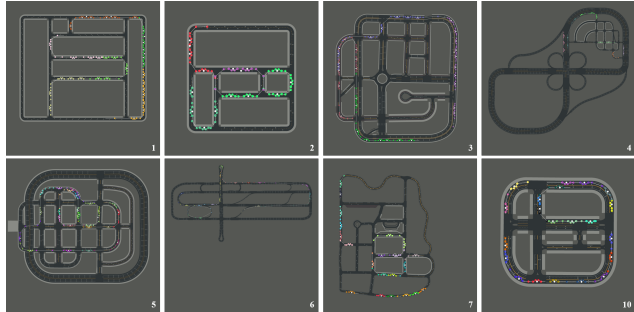


Figure 4. Town routes (Train: 1–4, Val.: 5, 6, Test: 7, 10) in the CARLA Simulator. Note that only one sample from each town is shown.

The specific parameters tuned for each condition are outlined in *Supplementary*, while the remaining fog density, distance, falloff, wetness parameters are set to zero.

Dataset Split. AVOID is split into three subsets; the training and validation subsets respectively are derived from the train and validation subsets of the Longest6 benchmark [13], with obstacles appearing in the driving scenes overlapping in train and validation subsets. The test subset contains paths from the Towns 7 and 10 from the eight CARLA towns, containing obstacles that are not part of either train or validation. The Longest6 benchmark contains 1.5 km long routes, higher traffic density, and challenging traffic scenarios set by the authors, from which we selected a smaller portion among the available towns 1-6 excluding areas of infeasible waypoint routes by the vehicle upon observing an obstacle. The waypoints for navigation in the test scenarios were all hand-labeled to specifically design challenging paths containing the obstacles that do not appear in the other two subsets. This allows for evaluating the capability of a navigation model to detect even untrained obstacles. In each of the train-val/test subsets, we introduce 39/6 unique obstacles which are described in detail in *Supplementary*.

4. Single-task Benchmark Evaluation

4.1. Supervised Semantic Segmentation on AVOID

As AVOID is designed to incorporate obstacles of various characteristics for detection from the segmentation map, it supports the standard semantic segmentation task. All benchmark results on high-performing semantic segmentation methods evaluated on the test set of AVOID are reported in Table 3, and the detailed per-class results for the state-of-the-art obstacle detection networks are reported in Table 2. While the current state-of-the-art obstacle detection network, RODSNet, achieves the highest overall mIoU across all 17 tested classes, RODSNet with a waypoint prediction network (GRU) outperforms for the obstacle class.

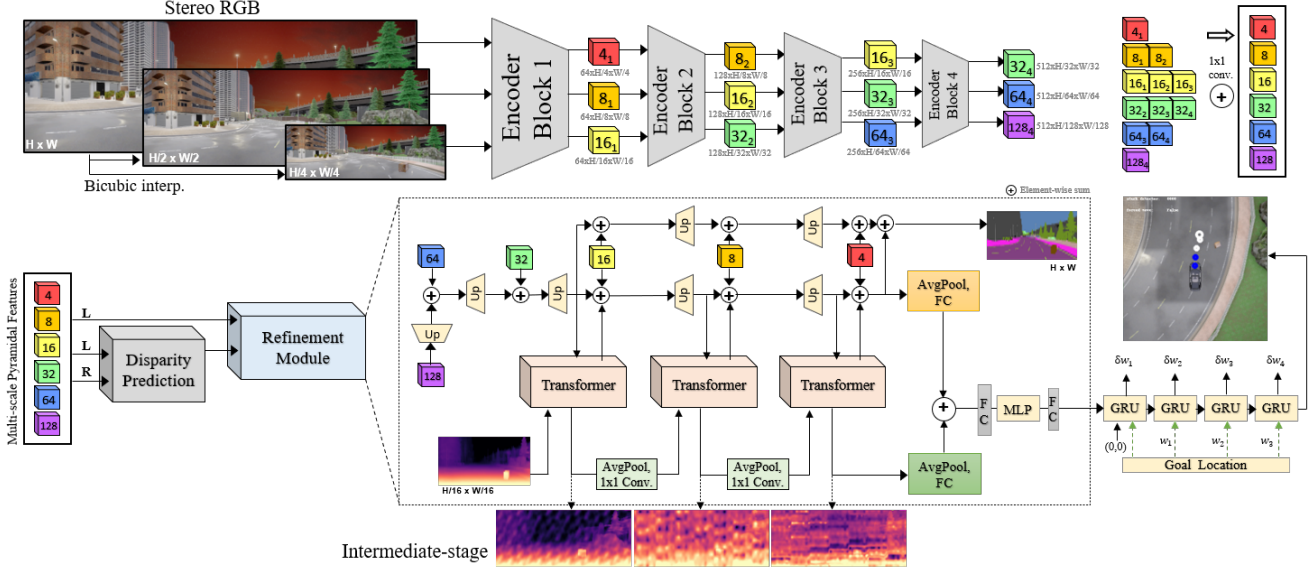


Figure 5. Overall network architecture of our multi-modal (RGB-D) transformer-based fusion network for multi-task learning, called SwiftFuser. We compare this network to RODSNet with GRU added for waypoint prediction, in which initial semantic and disparity maps are each averaged pooled and input to the GRU modules.

Our experimented SwiftFuser model yields the second-best score for the obstacle class, while achieving a comparable overall mIoU. We highlight that the segmentation results for *pedestrian* and *traffic light for stopping* are close to zero due to few occurrences of such class objects encountered before the vehicle throughout the test dataset.

Evaluation Metric. We evaluate the semantic segmentation performance quantitatively by the Intersection-over-Union (IoU) metric. IoU, or commonly the Jaccard index, accounts for the ratio of the area of overlap to union between the predicted and the ground truth image pixels as described in Eq. 1.

$$IoU = \frac{TP}{TP + FP + FN}, \quad (1)$$

where TP, FP, FN, respectively, denote true positive, false positive, and false negative pixels. The class-averaged IoU is represented as the mean IoU, or mIoU.

4.2. Waypoint Prediction

Waypoint prediction is defined as the task of navigating through the pre-defined set of routes. These route sequences contain sparse goal locations in GPS coordinates from the global planner, and the driving proficiency of an autonomous agent is evaluated based on these routes. Starting at an initial position, agents are to drive through the planned path to a destination point, where routes are derived from multiple domains, including freeways, urban scenes, and residential districts. Following the evaluation criteria from the Longest6 benchmark [13], we report the

two multi-modal fusion transformer network performance on our dataset in Table 4.

Evaluation Metrics. *Route completion (RC)* score is the percentage of route distances completed by the agent averaged across N routes, with the penalty 1(-% off route distance) given if the agent drives outside the planned route lanes for a percentage of the route (Eq. 2).

$$RC = \frac{1}{N} \sum_i R_i. \quad (2)$$

During the route a penalty is given to the agent, starting with an ideal 1.0 base score, as a geometric series of infraction penalty coefficients (p^j) for every infraction instance j , i.e., *Infraction Score (IS)* (Eq. 3). The pre-defined penalty coefficients for collisions with a pedestrian, a vehicle and static layout, and for red light violations are 0.50, 0.60, 0.65, and 0.7, respectively.

$$IS = \prod_j^{\text{Ped,Veh,Stat,Red}} (p^j)^{\text{infractions}^j}. \quad (3)$$

Driving Score (DS) is the averaged route completion (RC) with infraction multiplier P_i (Eq. 4):

$$DS = \frac{1}{N} \sum_i R_i P_i. \quad (4)$$

TransFuser is a recent network architecture for end-to-end driving consisting of multi-modal fusion transformer

Table 2. Per-class semantic segmentation IoU (%) results on test set of the AVOID dataset, averaged over all conditions. Class labels: Building, Fence, Pedestrian, Pole, Road Line, Road, Sidewalk, Vegetation, Vehicle, Wall, Sky, Terrain, Traffic Light for Stopping (Red/Yellow Light), Obstacle, Traffic Light for Proceeding (Traffic Light/Green Light), and Traffic Sign (from left to right). Best in **boldface**, runner-up in underline. See *Supplementary* for condition-specific results.

Method	Bui	Fen	Ped	Pol	RoLi	Roa	Sid	Veg	Veh	Wal	Sky	Ter	TL-s	Obs	TL-p	TS	mIoU
RFNet [70]	43.63	19.21	0.00	42.74	13.47	88.67	85.51	63.48	0.00	0.00	0.00	56.17	0.00	23.61	0.00	0.00	33.50
SwiftNet [†] [48]	<u>80.95</u>	3.93	0.00	27.94	54.22	89.40	68.62	69.47	8.59	1.93	92.67	43.38	0.00	<u>42.47</u>	16.11	6.79	36.59
RODSNet [†]	78.15	2.71	0.00	<u>30.65</u>	<u>60.80</u>	85.65	65.36	69.30	12.71	9.98	91.80	42.31	1.05	40.47	<u>19.90</u>	<u>13.12</u>	37.62
RODSNet [‡]	81.50	5.16	0.00	29.97	56.95	91.52	75.30	<u>69.46</u>	23.27	<u>5.19</u>	<u>92.50</u>	<u>46.17</u>	0.00	35.30	22.95	14.30	39.28
SwiftFuser [†]	80.65	<u>6.74</u>	0.00	28.90	64.31	<u>91.15</u>	<u>72.18</u>	68.41	<i>13.12</i>	1.28	92.86	42.32	0.00	51.81	19.33	7.89	<u>38.56</u>
RODSNet[†]+GRU	80.82	4.09	0.00	30.67	57.55	90.82	68.09	68.70	16.57	1.96	93.23	42.75	0.00	58.86	21.97	7.99	38.73

[†]ResNet-18, [‡]ResNet-34 backbone

Table 3. Real-time Validation and Test Semantic Segmentation Benchmark Results over all 17 classes and the obstacle class, in order of ascending test obstacle IoU.

Network	Val.		Test		Params (M)	Runtime (ms)
	mIoU	Obs. IoU	mIoU	Obs. IoU		
ESPNet [43]	38.08	21.88	27.83	15.31	0.20	32
ENet [49]	43.73	37.93	33.30	15.56	0.35	86
MobileNetV3 [27]	31.70	22.83	25.57	16.61	3.18	48
LiteSeg [†] [21]	41.17	37.15	29.02	17.60	3.51	69
CGNet [75]	48.29	48.31	32.79	21.54	0.50	73
EDANet [39]	49.18	55.21	34.53	21.67	0.69	43
DenseNet* [34]	44.56	42.47	29.37	21.81	10.31	110
RPNNet [11]	43.93	30.19	32.37	25.08	1.89	60
FSFNet [33]	44.06	45.20	33.73	26.24	0.83	43
LiteSeg [†] [21]	51.44	58.60	34.39	28.33	20.55	50
FC-HardNet [6]	47.29	53.88	32.60	28.51	4.12	9
FasterSeg [10]	44.21	43.41	28.70	29.44	5.67	46
ERFNet [58]	49.15	55.76	37.02	30.58	2.07	53
DeeplabV1 [8]	49.23	57.90	33.44	33.19	20.50	30
LiteSeg* [21]	44.73	46.61	32.23	34.03	4.38	50
FCN [40]	60.71	38.59	38.59	34.94	18.64	22
DeeplabV3 [9]	43.67	49.31	30.64	40.32	39.04	7
SegNet [3]	57.91	62.85	36.49	40.60	29.45	5
DenseASPP [77]	50.57	60.96	34.77	42.05	10.22	12
PSPNet [82]	54.41	71.87	36.40	47.37	65.47	62
SwiftNet [48]	55.96	67.77	36.11	47.51	12.06	33
ESANet [⊕] [65]	65.41	87.85	41.53	48.80	23.94	10
BiSeNet [78]	53.15	64.64	35.34	51.23	12.56	6

[†]ShuffleNet [81] [‡]DarkNet-19 [55] * MobileNet V2 [64] [⊕] Ladder-style [⊕] RGB-D

blocks across image and LiDAR representations, and an auto-regressive waypoint prediction network. Its success in road navigation using image and LiDAR data with the auxiliary task losses, such as those accounting for semantic segmentation and depth estimation, closely resembles and motivated our approach of refining the predicted image and depth representations. In their architecture, the respective representations from each modality are sequentially fused via a transformer (GPT) block, whose outputs are then added back to the respective input features. This stage is repeated four times and the final image and LiDAR representations are element-wise summed to feed into the auto-regressive waypoint prediction network. As a baseline comparison, the authors also introduce Latent TransFuser which replaces the 2-channel LiDAR histogram input (BEV) with an equal channel positional embedding of the

same dimensions ($256 \times 256 \times 2$), whose values for the left-right and top-down axes each equally range from -1 to 1 in a single channel.

For the waypoint prediction task on, we compared the TransFuser-based models along with our experimented models in Table 4. With image and LiDAR sensor data together in TransFuser, the results by the three metrics (DS, RC, IS) are higher by a large margin than those from LatentFuser. This insinuates the effectiveness of multi-modal feature fusion between image and LiDAR data using our dataset as well, in addition to their tested Town05 benchmark. Using our transformer-based fusion refinement, the route navigation scores are even higher. In particular, the higher route completion score indicates that SwiftFuser is capable of avoiding obstacles and arrive at the destination points more effectively. RODSNet+GRU is a based on refinement using a stacked hourglass structure followed by an auto-regressive waypoint prediction network with the fused representations as its input. We observed that a stacked hourglass structure may be more effective than the one-way transformer-based cross-modal learning in SwiftFuser.

Table 4. Route navigation benchmark test results evaluated on the test set of AVOID.

Waypoint Prediction Model	DS \uparrow	RC \uparrow	IS \uparrow
Latent TransFuser [13]	79.40	86.41	0.88
TransFuser [13]	88.82	96.03	0.91
SwiftFuser	94.22	98.07	0.95
RODSNet [67]+GRU	97.14	100.00	0.97
Expert (Oracle)	97.86	100.00	0.98

5. Multi-task Learning on AVOID

5.1. Overview

We propose to examine the effect of transformer-based feature refinement against the stacked hourglass-style refinement as practiced in RODSNet [67]. As in Fig. 5, we

- fic network. In *Proceedings of the IEEE/CVF international conference on computer vision*, pages 3552–3561, 2019. 7
- [7] Dian Chen, Brady Zhou, Vladlen Koltun, and Philipp Krähenbühl. Learning by cheating. In *Conference on Robot Learning*, pages 66–75. PMLR, 2020. 4
- [8] Liang-Chieh Chen, George Papandreou, Iasonas Kokkinos, Kevin Murphy, and Alan L. Yuille. Deeplab: Semantic image segmentation with deep convolutional nets, atrous convolution, and fully connected crfs. *IEEE Transactions on Pattern Analysis and Machine Intelligence*, 40(4):834–848, 2018. 7
- [9] Liang-Chieh Chen, George Papandreou, Florian Schroff, and Hartwig Adam. Rethinking atrous convolution for semantic image segmentation. 2017. 7
- [10] Wuyang Chen, Xinyu Gong, Xianming Liu, Qian Zhang, Yuan Li, and Zhangyang Wang. FASTERseg: Searching for faster real-time semantic segmentation. 2019. 7
- [11] Xiaoyu Chen, Xiaotian Lou, Lianfa Bai, and Jing Han. Residual pyramid learning for single-shot semantic segmentation. *IEEE Transactions on Intelligent Transportation Systems*, 21(7):2990–3000, 2019. 7
- [12] Kashyap Chitta, Aditya Prakash, and Andreas Geiger. Neat: Neural attention fields for end-to-end autonomous driving. In *International Conference on Computer Vision (ICCV)*, 2021. 3
- [13] Kashyap Chitta, Aditya Prakash, Bernhard Jaeger, Zehao Yu, Katrin Renz, and Andreas Geiger. Transfuser: Imitation with transformer-based sensor fusion for autonomous driving. *Pattern Analysis and Machine Intelligence (PAMI)*, 2022. 2, 3, 4, 5, 6, 7, 8
- [14] Marius Cordts, Mohamed Omran, Sebastian Ramos, Timo Rehfeld, Markus Enzweiler, Rodrigo Benenson, Uwe Franke, Stefan Roth, and Bernt Schiele. The cityscapes dataset for semantic urban scene understanding. In *Proceedings of the IEEE Conference on Computer Vision and Pattern Recognition (CVPR)*, June 2016. 2, 3, 4
- [15] Paulo Costa, Hugo Fernandes, Paulo Martins, João Barroso, and Leontios J Hadjileontiadis. Obstacle detection using stereo imaging to assist the navigation of visually impaired people. *Procedia Computer Science*, 14:83–93, 2012. 2
- [16] Clement Creusot and Asim Munawar. Real-time small obstacle detection on highways using compressive rbm road reconstruction. In *2015 IEEE Intelligent Vehicles Symposium (IV)*, pages 162–167. IEEE, 2015. 2
- [17] Dengxin Dai, Christos Sakaridis, Simon Hecker, and Luc Van Gool. Curriculum model adaptation with synthetic and real data for semantic foggy scene understanding. *International Journal of Computer Vision*, 128(5):1182–1204, 2020. 3
- [18] Dengxin Dai and Luc Van Gool. Dark model adaptation: Semantic image segmentation from daytime to nighttime. In *2018 21st International Conference on Intelligent Transportation Systems (ITSC)*, pages 3819–3824. IEEE, 2018. 3
- [19] Jean-Emmanuel Deschaud, David Duque, Jean Pierre Richa, Santiago Velasco-Forero, Beatriz Marcotegui, and François Goulette. Paris-carla-3d: A real and synthetic outdoor point cloud dataset for challenging tasks in 3d mapping. *Remote Sensing*, 13(22), 2021. 3
- [20] Alexey Dosovitskiy, German Ros, Felipe Codevilla, Antonio Lopez, and Vladlen Koltun. CARLA: An open urban driving simulator. In *Proceedings of the 1st Annual Conference on Robot Learning*, pages 1–16, 2017. 2, 3, 4, 5
- [21] Taha Emara, Hossam E Abd El Munim, and Hazem M Abbas. LiteSeg: A novel lightweight convnet for semantic segmentation. In *2019 Digital Image Computing: Techniques and Applications (DICTA)*, pages 1–7. IEEE, 2019. 7
- [22] Yuhua Fan, Luping Zhou, Liya Fan, and Jing Yang. Multiple obstacle detection for assistance driver system using deep neural networks. In *International Conference on Artificial Intelligence and Security*, pages 501–513. Springer, 2019. 2
- [23] DOT Federal Motor Carrier Safety Administration (FMCSA). 49 cfr parts 385 and 395. hours of service of drivers. Docket No. FMCSA-2018-0248, 2020 [Online]. 2
- [24] Andreas Geiger, Philip Lenz, and Raquel Urtasun. Are we ready for autonomous driving? the kitti vision benchmark suite. In *2012 IEEE conference on computer vision and pattern recognition*, pages 3354–3361. IEEE, 2012. 2
- [25] Shivani Godha. On-road obstacle detection system for driver assistance. *Asia Pacific Journal of Engineering Science and Technology*, 3(1):16–21, 2017. 2
- [26] H. Hirschmuller. Accurate and efficient stereo processing by semi-global matching and mutual information. In *2005 IEEE Computer Society Conference on Computer Vision and Pattern Recognition (CVPR)*, volume 2, pages 807–814, 2005. 4
- [27] Andrew Howard, Mark Sandler, Grace Chu, Liang-Chieh Chen, Bo Chen, Mingxing Tan, Weijun Wang, Yukun Zhu, Ruoming Pang, Vijay Vasudevan, et al. Searching for mobilenetv3. In *Proceedings of the IEEE/CVF international conference on computer vision*, pages 1314–1324, 2019. 7
- [28] Xinyu Huang, Peng Wang, Xinjing Cheng, Dingfu Zhou, Qichuan Geng, and Ruigang Yang. The apollo-scape open dataset for autonomous driving and its application. *IEEE transactions on pattern analysis and machine intelligence*, 42(10):2702–2719, 2019. 3
- [29] Loay Ismail, Lubna Eliyan, Razan Younes, and Reem Ahmed. Monocular vision-based collision avoidance system using shadow detection. In *2013 7th IEEE GCC Conference and Exhibition (GCC)*, pages 589–594. IEEE, 2013. 2
- [30] Matthew Johnson-Roberson, Charles Barto, Rounak Mehta, Sharath Nittur Sridhar, Karl Rosaen, and Ram Vasudevan. Driving in the matrix: Can virtual worlds replace human-generated annotations for real world tasks? In *2017 IEEE International Conference on Robotics and Automation (ICRA)*, page 746–753. IEEE Press, 2017. 3
- [31] Mourad A Kenk and Mahmoud Hassaballah. Dawn: vehicle detection in adverse weather nature dataset. *arXiv preprint arXiv:2008.05402*, 2020. 3
- [32] Abdulrahman Kerim, Felipe Chamone, Washington Ramos, Leandro Soriano Marcolino, Erickson R. Nascimento, and Richard Jiang. Semantic segmentation under adverse conditions: A weather and nighttime-aware synthetic data-based approach. 2022. 2
- [33] Minjong Kim, Byungjae Park, and Suyoung Chi. Accelerator-aware fast spatial feature network for real-time

- semantic segmentation. *IEEE Access*, 8:226524–226537, 2020. 7
- [34] Ivan Krešo, Josip Krapac, and Siniša Šegvić. Efficient ladder-style densenets for semantic segmentation of large images. *IEEE Transactions on Intelligent Transportation Systems*, 22(8):4951–4961, 2020. 7
- [35] Balaji Lakshminarayanan, Alexander Pritzel, and Charles Blundell. Simple and scalable predictive uncertainty estimation using deep ensembles. *Advances in neural information processing systems*, 30, 2017. 2
- [36] Dan Levi, Noa Garnett, Ethan Fetaya, and Israel Herzlyia. Stixelnet: A deep convolutional network for obstacle detection and road segmentation. In *BMVC*, volume 1, page 4, 2015. 2
- [37] Krzysztof Lis, Sina Honari, Pascal Fua, and Mathieu Salzmann. Perspective aware road obstacle detection. *arXiv preprint arXiv:2210.01779*, 2022. 2
- [38] Krzysztof Lis, Krishna Nakka, Pascal Fua, and Mathieu Salzmann. Detecting the unexpected via image resynthesis. In *Proceedings of the IEEE/CVF International Conference on Computer Vision*, pages 2152–2161, 2019. 2
- [39] Shao-Yuan Lo, Hsueh-Ming Hang, Sheng-Wei Chan, and Jing-Jih Lin. Efficient dense modules of asymmetric convolution for real-time semantic segmentation. In *Proceedings of the ACM Multimedia Asia*, pages 1–6, 2019. 7
- [40] Jonathan Long, Evan Shelhamer, and Trevor Darrell. Fully convolutional networks for semantic segmentation. In *Proceedings of the IEEE conference on computer vision and pattern recognition*, pages 3431–3440, 2015. 7
- [41] Guanglin Ma, Manoj Dwivedi, Ran Li, Chong Sun, and Anton Kummert. A real-time rear view camera based obstacle detection. In *2009 12th International IEEE Conference on Intelligent Transportation Systems*, pages 1–6. IEEE, 2009. 2
- [42] Colin D. Mathers, Christina Bernard, Kim Moesgaard Iburg, Mie Inoue, Doris Ma Fat, Kenji Shibuya, Claudia Stein, Niels Tomijima, and Hongyi Xu. Global burden of disease in 2002: data sources, methods and results. Technical report, World Health Organization, Geneva 27, Switzerland, 12 2003. <https://www.who.int/healthinfo/paper54.pdf>. 1
- [43] Sachin Mehta, Mohammad Rastegari, Anat Caspi, Linda Shapiro, and Hannaneh Hajishirzi. Espnet: Efficient spatial pyramid of dilated convolutions for semantic segmentation. In *Proceedings of the european conference on computer vision (ECCV)*, pages 552–568, 2018. 7
- [44] Valentina Muşat, Ivan Fursa, Paul Newman, Fabio Cuzzolin, and Andrew Bradley. Multi-weather city: Adverse weather stacking for autonomous driving. In *Proceedings of the IEEE/CVF International Conference on Computer Vision*, pages 2906–2915, 2021. 3
- [45] Gerhard Neuhold, Tobias Ollmann, Samuel Rota Buló, and Peter Kotschieder. The mapillary vistas dataset for semantic understanding of street scenes. In *Proceedings of the IEEE international conference on computer vision*, pages 4990–4999, 2017. 3
- [46] Toshiaki Ohgushi, Kenji Horiguchi, and Masao Yamanaka. Road obstacle detection method based on an autoencoder with semantic segmentation. In *Proceedings of the Asian Conference on Computer Vision*, 2020. 2
- [47] World Health Organization. Road traffic injuries. Technical report, World Health Organization, Geneva 27, Switzerland, 2021. 1
- [48] Marin Oršić and Siniša Šegvić. Efficient semantic segmentation with pyramidal fusion. *Pattern Recognition*, 110:107611, 2021. 7
- [49] Adam Paszke, Abhishek Chaurasia, Sangpil Kim, and Eugenio Culurciello. Enet: A deep neural network architecture for real-time semantic segmentation. *arXiv preprint arXiv:1606.02147*, 2016. 7
- [50] Andreas Pfeuffer and Klaus Dietmayer. Robust semantic segmentation in adverse weather conditions by means of sensor data fusion. In *2019 22th International Conference on Information Fusion (FUSION)*, pages 1–8. IEEE, 2019. 3
- [51] Peter Pinggera, Uwe Franke, and Rudolf Mester. High-performance long range obstacle detection using stereo vision. In *2015 IEEE/RSJ International Conference on Intelligent Robots and Systems (IROS)*, pages 1308–1313. IEEE, 2015. 2
- [52] Peter Pinggera, Sebastian Ramos, Stefan Gehrig, Uwe Franke, Carsten Rother, and Rudolf Mester. Lost and found: detecting small road hazards for self-driving vehicles. In *2016 IEEE/RSJ International Conference on Intelligent Robots and Systems (IROS)*, pages 1099–1106. IEEE, 2016. 2, 4
- [53] Sebastian Ramos, Stefan Gehrig, Peter Pinggera, Uwe Franke, and Carsten Rother. Detecting unexpected obstacles for self-driving cars: Fusing deep learning and geometric modeling. In *2017 IEEE Intelligent Vehicles Symposium (IV)*, pages 1025–1032. IEEE, 2017. 2
- [54] Thiago Rateke and Aldo von Wangenheim. Passive vision road obstacle detection: a literature mapping. *International Journal of Computers and Applications*, 44(4):376–395, 2022. 2
- [55] Joseph Redmon. Darknet: Open source neural networks in c. <http://pjreddie.com/darknet/>, 2013–2016. 7
- [56] Stephan R Richter, Zeeshan Hayder, and Vladlen Koltun. Playing for benchmarks. In *Proceedings of the IEEE International Conference on Computer Vision*, pages 2213–2222, 2017. 3
- [57] Stephan R Richter, Vibhav Vineet, Stefan Roth, and Vladlen Koltun. Playing for data: Ground truth from computer games. In *European conference on computer vision*, pages 102–118. Springer, 2016. 3
- [58] Eduardo Romera, José M Alvarez, Luis M Bergasa, and Roberto Arroyo. Erfnet: Efficient residual factorized convnet for real-time semantic segmentation. *IEEE Transactions on Intelligent Transportation Systems*, 19(1):263–272, 2017. 2, 3, 7
- [59] Thomas Rothmeier and Werner Huber. Let it snow: On the synthesis of adverse weather image data. In *2021 IEEE International Intelligent Transportation Systems Conference (ITSC)*, pages 3300–3306. IEEE, 2021. 3
- [60] Christos Sakaridis, Dengxin Dai, and Luc Van Gool. Semantic foggy scene understanding with synthetic data. *Inter-*

- national Journal of Computer Vision*, 126(9):973–992, Sep 2018. [3](#)
- [61] Christos Sakaridis, Dengxin Dai, and Luc Van Gool. Map-guided curriculum domain adaptation and uncertainty-aware evaluation for semantic nighttime image segmentation. *IEEE Transactions on Pattern Analysis and Machine Intelligence*, 2020. [3](#)
- [62] Christos Sakaridis, Dengxin Dai, and Luc Van Gool. ACDC: The adverse conditions dataset with correspondences for semantic driving scene understanding. In *Proceedings of the IEEE/CVF International Conference on Computer Vision (ICCV)*, October 2021. [2](#), [3](#), [4](#)
- [63] Pouyan Salavati and Hossein Mahvash Mohammadi. Obstacle detection using googlenet. In *2018 8th International Conference on Computer and Knowledge Engineering (ICCKE)*, pages 326–332, 2018. [2](#)
- [64] Mark Sandler, Andrew Howard, Menglong Zhu, Andrey Zhmoginov, and Liang-Chieh Chen. Mobilenetv2: Inverted residuals and linear bottlenecks. In *Proceedings of the IEEE conference on computer vision and pattern recognition*, pages 4510–4520, 2018. [7](#)
- [65] Daniel Seichter, Mona Köhler, Benjamin Lewandowski, Tim Wengefeld, and Horst-Michael Gross. Efficient rgb-d semantic segmentation for indoor scene analysis. In *2021 IEEE International Conference on Robotics and Automation (ICRA)*, pages 13525–13531. IEEE, 2021. [7](#)
- [66] Marcel Sheeny, Emanuele De Pellegrin, Saptarshi Mukherjee, Alireza Ahrabian, Sen Wang, and Andrew Wallace. Radiate: A radar dataset for automotive perception in bad weather. In *2021 IEEE International Conference on Robotics and Automation (ICRA)*, pages 1–7. IEEE, 2021. [3](#)
- [67] Taek-Jin Song, Jongoh Jeong, and Jong-Hwan Kim. End-to-end real-time obstacle detection network for safe self-driving via multi-task learning. *IEEE Transactions on Intelligent Transportation Systems*, 23(9):16318–16329, 2022. [2](#), [3](#), [7](#), [8](#)
- [68] John M. Sullivan and Michael J. Flannagan. Determining the potential safety benefit of improved lighting in three pedestrian crash scenarios. *Accident Analysis & Prevention*, 39(3):638–647, 2007. [2](#)
- [69] Lei Sun, Kailun Yang, Xinxin Hu, Weijian Hu, and Kaiwei Wang. Real-time fusion network for rgb-d semantic segmentation incorporating unexpected obstacle detection for road-driving images. *IEEE Robotics and Automation Letters*, 5(4):5558–5565, 2020. [2](#)
- [70] Lei Sun, Kailun Yang, Xinxin Hu, Weijian Hu, and Kaiwei Wang. Real-time fusion network for rgb-d semantic segmentation incorporating unexpected obstacle detection for road-driving images. *IEEE Robotics and Automation Letters*, 5(4):5558–5565, 2020. [7](#)
- [71] Tao Sun, Mattia Segu, Janis Postels, Yuxuan Wang, Luc Van Gool, Bernt Schiele, Federico Tombari, and Fisher Yu. SHIFT: a synthetic driving dataset for continuous multi-task domain adaptation. In *Proceedings of the IEEE/CVF Conference on Computer Vision and Pattern Recognition (CVPR)*, pages 21371–21382, June 2022. [4](#)
- [72] Xiaoyang Tan, Ziyi Wang, and Changhao Piao. Road obstacle detection algorithm based on lidar point cloud. In *Second International Conference on Sensors and Information Technology (ICSI 2022)*, volume 12248, pages 296–302. SPIE, 2022. [2](#)
- [73] B.C Tefft. The prevalence of motor vehicle crashes involving road debris, united states, 2011-2014. Technical report, AAA Foundation for Traffic Safety, Washington, D.C., 2016. [1](#)
- [74] Frederick Tung, Jianhui Chen, Lili Meng, and James J Little. The raincouver scene parsing benchmark for self-driving in adverse weather and at night. *IEEE Robotics and Automation Letters*, 2(4):2188–2193, 2017. [3](#)
- [75] Tianyi Wu, Sheng Tang, Rui Zhang, Juan Cao, and Yongdong Zhang. Cgnet: A light-weight context guided network for semantic segmentation. *IEEE Transactions on Image Processing*, 30:1169–1179, 2020. [7](#)
- [76] Haofei Xu and Juyong Zhang. Aanet: Adaptive aggregation network for efficient stereo matching. In *Proceedings of the IEEE/CVF Conference on Computer Vision and Pattern Recognition*, pages 1959–1968, 2020. [8](#)
- [77] Maoke Yang, Kun Yu, Chi Zhang, Zhiwei Li, and Kuiyuan Yang. Denseaspp for semantic segmentation in street scenes. In *Proceedings of the IEEE conference on computer vision and pattern recognition*, pages 3684–3692, 2018. [7](#)
- [78] Changqian Yu, Jingbo Wang, Chao Peng, Changxin Gao, Gang Yu, and Nong Sang. Bisenet: Bilateral segmentation network for real-time semantic segmentation. In *Proceedings of the European conference on computer vision (ECCV)*, pages 325–341, 2018. [7](#)
- [79] Fisher Yu, Haofeng Chen, Xin Wang, Wenqi Xian, Yingying Chen, Fangchen Liu, Vashisht Madhavan, and Trevor Darrell. Bdd100k: A diverse driving dataset for heterogeneous multitask learning. In *Proceedings of the IEEE/CVF conference on computer vision and pattern recognition*, pages 2636–2645, 2020. [3](#)
- [80] Oliver Zendel, Katrin Honauer, Markus Murschitz, Daniel Steininger, and Gustavo Fernandez Dominguez. Wilddash-creating hazard-aware benchmarks. In *Proceedings of the European Conference on Computer Vision (ECCV)*, pages 402–416, 2018. [3](#)
- [81] Xiangyu Zhang, Xinyu Zhou, Mengxiao Lin, and Jian Sun. Shufflenet: An extremely efficient convolutional neural network for mobile devices. In *Proceedings of the IEEE conference on computer vision and pattern recognition*, pages 6848–6856, 2018. [7](#)
- [82] Hengshuang Zhao, Jianping Shi, Xiaojuan Qi, Xiaogang Wang, and Jiaya Jia. Pyramid scene parsing network. In *Proceedings of the IEEE conference on computer vision and pattern recognition*, pages 2881–2890, 2017. [7](#)